



**HAL**  
open science

## Quantitative fluorescence diffuse optical tomography in the presence of heterogeneities

Teresa Correia, Nicolas Ducros, Cosimo d'Andrea, Martin Schweiger, Simon Arridge

► **To cite this version:**

Teresa Correia, Nicolas Ducros, Cosimo d'Andrea, Martin Schweiger, Simon Arridge. Quantitative fluorescence diffuse optical tomography in the presence of heterogeneities. *Optics Letters*, 2013, 38 (11), pp.1903–1905. 10.1364/OL.38.001903 . hal-00875155

**HAL Id: hal-00875155**

**<https://hal.science/hal-00875155>**

Submitted on 21 Oct 2013

**HAL** is a multi-disciplinary open access archive for the deposit and dissemination of scientific research documents, whether they are published or not. The documents may come from teaching and research institutions in France or abroad, or from public or private research centers.

L'archive ouverte pluridisciplinaire **HAL**, est destinée au dépôt et à la diffusion de documents scientifiques de niveau recherche, publiés ou non, émanant des établissements d'enseignement et de recherche français ou étrangers, des laboratoires publics ou privés.

# Quantitative fluorescence diffuse optical tomography in the presence of heterogeneities

Teresa Correia,<sup>1,\*</sup> Nicolas Ducros,<sup>2</sup> Cosimo D'Andrea,<sup>2,3</sup> Martin Schweiger,<sup>1</sup> and Simon Arridge<sup>1</sup>

<sup>1</sup>Department of Computer Science, University College London, Gower Street, London WC1E 6BT, UK

<sup>2</sup>IFN-CNR, Dipartimento di Fisica, Politecnico di Milano, Piazza Leonardo da Vinci 32, Milan I-20133, Italy

<sup>3</sup>CNST of IIT@polimi, Via Pascoli 70/3, Milano 20133, Italy

\*Corresponding author: t.correia@ucl.ac.uk

Received December 26, 2012; revised February 22, 2013; accepted May 1, 2013;  
posted May 2, 2013 (Doc. ID 182220); published May 27, 2013

In fluorescence diffuse optical tomography (fDOT), the accuracy of reconstructed fluorescence distributions highly depends on the knowledge of the tissue optical heterogeneities for correct modeling of light propagation. Common approaches are to assume homogeneous optical properties or, when structural information is available, assign optical properties to various segmented organs, which is likely to result in inaccurate reconstructions. Furthermore, DOT based only on intensity (continuous wave-DOT) is a nonunique inverse problem, and hence, cannot be used to retrieve simultaneously maps of absorption and diffusion coefficients. We propose a method that reconstructs a single parameter from the excitation measurements, which is used in the fDOT problem to accurately recover fluorescence distribution. © 2013 Optical Society of America

OCIS codes: (170.0170) Medical optics and biotechnology; (110.3010) Image reconstruction techniques.

<http://dx.doi.org/10.1364/OL.38.001903>

Fluorescence diffuse optical tomography (fDOT) is an imaging modality that has become increasingly popular for monitoring molecular and cellular activity in small animals [1]. In fDOT, maps of the fluorescence distribution are produced from intensity measurements of near-infrared light. However, the quality of the reconstructed images depends on how accurately the tissue optical heterogeneity is modeled. Soubret *et al.* [2] suggested the normalized Born approximation approach to deal with the optical heterogeneity of tissue. Recently, fDOT systems have been combined with an anatomical imaging modality, most commonly x-ray computed tomography, which provides information about the internal structure, and optical properties, obtained from the literature or experimentally, can be assigned to the different tissue types, improving the quality of the reconstructions [3,4]. Another approach is to use diffuse optical tomography (DOT) to estimate the optical property distribution within the medium [5,6]. However, continuous wave (CW) DOT at a single wavelength is a nonunique problem, meaning that simultaneous recovery of diffusion and absorption coefficients is not feasible [7]. The non-uniqueness arguments have also been extended to fDOT [8]. Thus, several sets of fluorescence yield, absorption, and scattering coefficients can lead to the same measurements. Here we introduce a strategy to determine tissue heterogeneities in fDOT and, if available, include *a priori* anatomical information into the image reconstruction.

The forward problem in CW-fDOT is to model the propagation of light described by the following set of equations in domain  $\Omega$

$$-\nabla \cdot \kappa^e \nabla \Phi^e + \mu_a^e \Phi^e = 0, \quad (1)$$

$$-\nabla \cdot \kappa^f \nabla \Phi^f + \mu_a^f \Phi^f = \Phi^e h \quad (2)$$

with boundary conditions on  $\partial\Omega$

$$\Phi^e + 2R\kappa^e \hat{n} \cdot \nabla \Phi^e = J^-, \quad (3)$$

$$\Phi^f + 2R\kappa^f \hat{n} \cdot \nabla \Phi^f = 0, \quad (4)$$

$$\Gamma^{e,f} = -\kappa^{e,f} \hat{n} \cdot \nabla \Phi^{e,f}, \quad (5)$$

where  $J^-$  is the excitation source flux,  $\Phi$  is the photon density,  $h$  is the fluorescence yield,  $R$  is a boundary term that incorporates the refractive index mismatch,  $\Gamma$  is the boundary measurement on  $\partial\Omega$ , and  $\hat{n}$  is the outer normal vector. The diffusion coefficient is given by  $\kappa = (1/3)(\mu_s' + \mu_a)^{-1}$ , where  $\mu_a$  and  $\mu_s'$  are the absorption and reduced scattering coefficients, respectively, and superscript  $e, f$  indicates the excitation and emission wavelengths  $\lambda^e, \lambda^f$ , respectively.

The inverse problem of CW-fDOT is to solve  $\Gamma^f = F(h, \mu_a, \kappa)$ . If  $\mu_a$  and  $\kappa$  are assumed to be known, only  $h$  is recovered. This becomes a linear problem

$$\Gamma^f = Ah. \quad (6)$$

Following the derivation in [7], the system Eqs. (1)–(5) are transformable to the Helmholtz type using the change of variables  $\gamma^2 = \kappa$ ,  $\Psi = \gamma\Phi$ , and  $\eta = (\nabla^2\gamma/\gamma) + (\mu_a/\gamma^2)$ , leading to

$$-\nabla^2\Psi^e + \eta^e\Psi^e = 0, \quad (7)$$

$$-\nabla^2\Psi^f + \eta^f\Psi^f = \Psi^e \frac{h}{\gamma^f \gamma^e}, \quad (8)$$

in  $\Omega$  and

$$\Psi^e + 2R\kappa^e \hat{n} \cdot \nabla \Psi^e = \gamma^e J^-, \quad (9)$$

$$\Psi^f + 2R\kappa^f \hat{n} \cdot \nabla \Psi^f = 0, \quad (10)$$

$$\Gamma^{e,f} = -\gamma^{e,f} \hat{n} \cdot \nabla \Psi^{e,f}, \quad (11)$$

in  $\partial\Omega$ , where we assume the normal derivative  $\hat{n} \cdot \nabla \gamma^{e,f} = 0$ .

The system Eqs. (7)–(11) are posed in terms of a new variable defined as

$$\Upsilon = \frac{h}{\gamma^f \gamma^e}. \quad (12)$$

We define the pair of inverse problems

$$\Gamma^e = F(\eta^e), \quad (13)$$

$$\Gamma^f = A(\Upsilon). \quad (14)$$

If  $\gamma^{e,f}$ ,  $\eta^{e,f}$  are assumed to be known everywhere in  $\Omega$ , then the recovery of  $\Upsilon$  from Eq. (14) has a unique solution if data  $\Gamma^f$  is measured for all possible source functions  $J^-$ . The use of normalized data  $\hat{\Gamma} = \Gamma^f / \Gamma^e$  allows uncertainty in estimating the absolute source power to be eliminated up to a multiplicative constant [2], but does not compensate for the effect of unknown optical parameter heterogeneity.

In this Letter, we propose to solve for  $\eta^e$  from measurements of  $\Gamma^e$  using nonlinear reconstruction, Eq. (13), followed by linear reconstruction of  $\Upsilon$  from normalized data  $\hat{\Gamma}$ , Eq. (14). Note that  $\Gamma^f$  in Eqs. (6) and (14) is replaced by  $\hat{\Gamma}$ . For simplicity, we assume optical parameters to be the same at  $\lambda^e$  and  $\lambda^f$ . This assumption could be relaxed if an additional measurement of transmitted intensity were made for sources at  $\lambda^f$ . In addition, we consider the application of tissue boundary information by modeling piecewise constant values of  $\eta$  in different tissues. In this case, the effect of incorrectly known tissue values needs to be considered.

We evaluated the performance of our method through a simulation study. We considered a medium with three

**Table 1. Optical Properties for the Three Different Tissue Types Used in the Simulation**

	True/Incorrect	
	$\mu_a$ (mm <sup>-1</sup> )	$\mu'_s$ (mm <sup>-1</sup> )
Skin/Muscle	0.018/0.028	1.23/1.0
Lungs	0.033/0.079	2.21/2.0
Heart	0.019/0.026	1.10/0.76

different tissues (lungs, heart, and skin/muscle). The geometry and the three fluorescent inclusions used in the simulation are shown in Fig. 1(a). We used a finite element implementation of the diffusion equation and Helmholtz-type equation [9]. The mesh used in the simulation had 29,172 nodes, 143,963 element and dimensions 58 mm × 58 mm × 63 mm. The 48 sources and 48 detectors were evenly distributed in 3 rings (16 sources and 16 detectors per ring) around the cylinder at  $z = \{-10, 0, 10\}$ , making a total of 2304 measurements. Data were simulated according to Eqs. (1) and (2), using the true optical properties in Table 1. Refractive index was considered to be 1.4, and 1% Gaussian noise was added to both excitation and emission measurements. The nonlinear problem in Eq. (13) was solved using an iteratively Tikhonov-regularized Gauss–Newton method [10], after which the reconstruction of  $\Upsilon$  from normalized data  $\hat{\Gamma}$  was solved from Eq. (14) with a single linear inversion step. Spatial structural information can be included by averaging within tissue regions the recovered  $\eta$  prior to the linear reconstruction step. Estimation of  $h$  from Eq. (12) depends critically on the estimation of  $\gamma^{e,f}$ , which is not possible with CW data. Therefore, we use the approximate diffusion coefficient  $\hat{\kappa} = (\mu_a^0 / \eta)$ , where  $\mu_a^0$  is an estimate of the (homogeneous) background absorption, since this quantity is also unknown.

In summary, our method consists of the following steps:

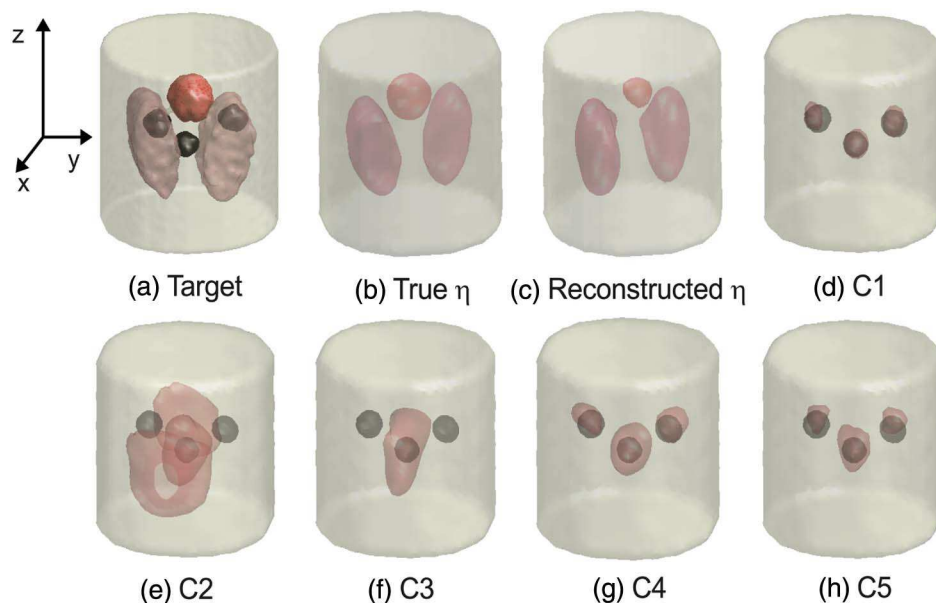


Fig. 1. (a) Simulation geometry showing three fluorescent targets (dark spheres), heart and lung shaped structures. (b) True and (c) reconstructed  $\eta$ . (d)–(h) Fluorescence distribution reconstructed using methods C1–C5, where the dark spheres represent the true solution.

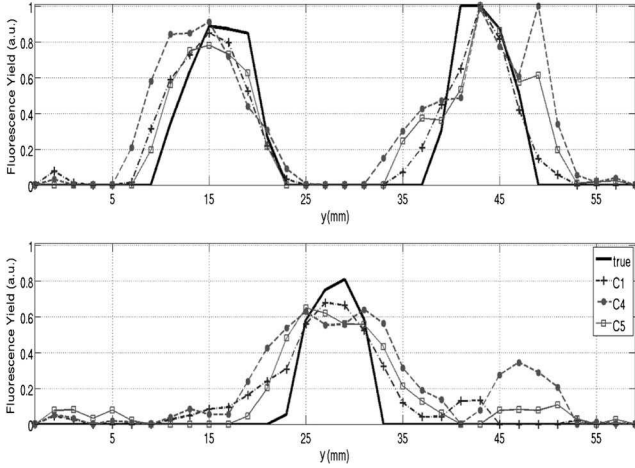


Fig. 2. Cross-sectional plots: (top) along the center of the two top fluorescent inclusions and (bottom) along the center of the bottom inclusion.

(1) Nonlinear reconstruction of  $\eta$  from  $\Gamma^e$  by solving Eq. (13);

(2) If structural information is to be included,  $\eta$  values are averaged and assigned to the different tissues:  $\eta_{\text{tissue}} = (1/N) \sum_i \eta_i \in \Omega_{\text{tissue}}$ , where  $N$  is the number of elements within the tissue domain  $\Omega_{\text{tissue}}$ ;

(3) Linear reconstruction of  $\Upsilon$  from  $\Gamma$  by solving Eq. (14);

(4) Recovery of fluorescence yield from  $h = \hat{\kappa}\Upsilon$ .

A few different cases were considered for comparison between the traditional method (cases 1 to 3) and the proposed method (cases 4 and 5):

C1 Solve Eq. (6) using the true optical properties;

C2 Solve Eq. (6) using homogeneous background (skin/muscle) optical properties;

C3 Solve Eq. (6) using the incorrect optical properties (Table 1);

C4 Our method, with  $\hat{\kappa} = (\mu_a^0/\eta)$ . Assuming  $\kappa^{e,f} = \kappa^{\text{true}}$  for the boundary conditions.

C5 As C4, with regional averaging of  $\eta$ .

Figure 1(b) shows the true  $\eta$  and Fig. 1(c) shows the reconstructed  $\eta$  (isosurfaces at half-maximum), which was used in Eq. (14) to reconstruct  $\Upsilon$  (step 3 of our method). Figures 1(d)–1(h) show the fluorescence distribution (isosurface at half-maximum) obtained with the different methods together with the true solution (dark spheres). Figure 1(d) shows the reconstructed fluorescent inclusions obtained using method C1, where the true optical properties were used in the forward model. This is the best estimate we can expect to obtain using fDOT. Figure 1(e) shows the solution obtained when homogeneous optical properties were used in the forward

model (method C2), where only the central inclusion was reconstructed in the correct location. Figure 1(f) shows the reconstructed fluorescence distribution obtained when the assigned optical properties are incorrect. Using our proposed method (C4), the inclusions are reconstructed in the correct location [Fig. 1(g)]. Using structural information and the averaged  $\eta$  values for the different tissues (method C5) results in a more accurate reconstruction of the size of the inclusions, as shown in Fig. 1(h).

Figure 2 shows the normalized cross-sectional plots, along the center of the spherical inclusions ( $y$  axis), of the true and reconstructed fluorescence distributions using methods C1, C4, and C5. The solid black line represents the true targets. Our method can recover with good accuracy the relative contrast among the targets.

We have proposed to use a Helmholtz-type equation, where the inverse problem involves the reconstruction of a single parameter,  $\eta$ , which depends on both the absorption and diffusion coefficients. The estimated heterogeneity map is used directly in the fDOT image reconstruction problem. Our method can recover the size, location, and relative concentration of the fluorescent objects with great accuracy, which can be further improved if structural information about the object of study is available. Note that the structural image does not provide information of fluorescent target location, only fDOT does. Even though one cannot obtain absolute fluorophore concentration values, relative values can be extremely useful for applications, such as monitoring tumor changes over time, treatment responses, and other disease-related changes in the molecular activity of specific areas.

## References

1. V. Ntziachristos, *Annu. Rev. Biomed. Eng.* **8**, 1 (2006).
2. A. Soubret, J. Ripoll, and V. Ntziachristos, *IEEE Trans. Med. Imag.* **24**, 1377 (2005).
3. D. Hyde, R. Schulz, D. Brooks, E. Miller, and V. Ntziachristos, *J. Opt. Soc. Am. A* **26**, 919 (2009).
4. W. Barber, Y. Lin, J. Iwanczyk, W. Roeck, O. Nalcioglu, and G. Gulsen, *Technol. Cancer Res. Treat.* **9**, 45 (2010).
5. L. Hervé, A. Koenig, A. Silva, M. Berger, J. Boutet, J. Dinten, P. Peltié, and P. Rizo, *Appl. Opt.* **46**, 4896 (2007).
6. Y. Lin, H. Yan, O. Nalcioglu, and G. Gulsen, *Appl. Opt.* **48**, 1328 (2009).
7. S. Arridge and W. Lionheart, *Opt. Lett.* **23**, 882 (1998).
8. L. Hervé, A. Koenig, and J.-M. Dinten, *J. Opt.* **13**, 015702 (2011).
9. M. Schweiger, S. Arridge, M. Hiraoka, and D. Delpy, *Med. Phys.* **22**, 1779 (1995).
10. M. Schweiger, S. Arridge, and I. Nissilä, *Phys. Med. Biol.* **50**, 2365 (2005).